

# Static and dynamic scattering from ternary polymer blends: Bicontinuous microemulsions, Lifshitz lines, and amphiphilicity<sup>a)</sup>

Terry L. Morkved,<sup>b)</sup> Petr Stepanek,<sup>c)</sup> Kasiraman Krishnan, Frank S. Bates, and Timothy P. Lodge<sup>d)</sup>

*Department of Chemical Engineering and Materials Science, University of Minnesota, Minneapolis, Minnesota 55455-0431*

(Received 27 November 2000; accepted 1 February 2001)

Ternary polymer blends, comprising two homopolymers and the corresponding diblock copolymer, have been examined by small-angle neutron scattering (SANS) and dynamic light scattering (DLS). Two chemical systems have been employed: one consisting of polyethylene, polydimethylsiloxane, and poly(ethylene-*b*-dimethylsiloxane), and another containing polyethylenepropylene, polyethyleneoxide, and poly(ethylenepropylene-*b*-ethylene oxide). The molecular weights and compositions were chosen to emphasize the region of the phase prism dominated by the bicontinuous microemulsion ( $B\mu E$ ) phase; the homopolymer molecular weights and volume fractions were approximately equal. The SANS intensity was compared quantitatively with the Teubner–Strey structure factor, and interpreted via the amphiphilicity factor  $f_a$ . The transition from a fully disordered mixture at higher temperatures to a well-developed  $B\mu E$  upon cooling did not correlate well with either the disorder line ( $f_a = +1$ ) or the total monomer Lifshitz line ( $f_a = 0$ ). However, DLS provided a clear signature of this transition, via a distinct maximum in the temperature dependence of the dynamic correlation length. We hypothesize that this maximum is closely correlated to the homopolymer/homopolymer Lifshitz line. The structure of the interfaces in the  $B\mu E$  was further examined in terms of the curvature and the copolymer coverage, as functions of copolymer concentration and temperature. © 2001 American Institute of Physics. [DOI: 10.1063/1.1357800]

## I. INTRODUCTION

Many applications of soft materials involve mixing otherwise incompatible molecules. Although a variety of equilibrium and nonequilibrium approaches are used to stabilize mixtures, the use of surfactants is particularly important. For example, in oil/water/surfactant (o/w/s) systems, both ionic and nonionic amphiphiles are used to confer thermodynamic stability.<sup>1,2</sup> These ternary or quaternary systems can form a plethora of ordered and disordered morphologies which depend on, *inter alia*, concentration, temperature, interfacial tension, and molecular size. Ordered states, such as lamellae, hexagonally packed cylinders, and cubic phases form in systems with strong amphiphilicity. As with most soft matter systems, there is a delicate balance between entropy and interfacial energy that controls ordering and mixing.<sup>2</sup> The interaction strength of the surfactant controls the degree of mixing, and thus it is important to quantify the amphiphilicity of the surfactant. Progress along these lines is impeded in part by the strong, asymmetric, and temperature-dependent interactions among the components.

Different polymer are also generally immiscible, at least

over some temperature range, and mixtures (“blends”) may be stabilized by various kinds of copolymer.<sup>3</sup> Most of the ordered and disordered phases identified in o/w/s systems have also been observed in the polymeric analogs. Of particular interest in this work is the bicontinuous microemulsion ( $B\mu E$ ).<sup>4</sup> A microemulsion is a structured fluid which is microscopically segregated but macroscopically disordered, with a vanishing interfacial tension between domains. In the o/w/s system, oil-rich and water-rich domains are separated by a surfactant-rich interface. In the ternary polymeric system, homopolymer-rich domains are separated by a block copolymer-rich interface. In addition to its potential technological applicability, the  $B\mu E$  provides an interesting model system with which the properties of low molecular weight and polymeric surfactants can be compared. In particular, the transition from a fully mixed, disordered phase to the structured, but still disordered  $B\mu E$  is challenging to describe theoretically. On the experimental side, the thermodynamic character and signatures of this transition are not yet established.

In this paper we present small angle neutron scattering (SANS) and dynamic light scattering (DLS) measurements on ternary polymer blends that exhibit the  $B\mu E$  phase. SANS permits demarcation of the disorder line and the total monomer Lifshitz line in the disordered phase, using the microemulsion model developed by Teubner and Strey.<sup>5</sup> Furthermore, the amphiphilicity may be quantified as a function of temperature and composition. However, the transition between a fully mixed disordered phase and the  $B\mu E$  is not

<sup>a)</sup>Dedicated to Professor Hans Sillescu on the occasion of his 65th birthday.

<sup>b)</sup>Current address: Imation Corporation, Oakdale, Minnesota 55128.

<sup>c)</sup>Also at: Institute of Macromolecular Chemistry, Czech Academy of Sciences, Prague, Czech Republic.

<sup>d)</sup>Author to whom correspondence should be addressed. Also at: Department of Chemistry, University of Minnesota, Minneapolis, Minnesota 55455; electronic mail: lodge@chem.umn.edu

clear. In contrast the DLS results, interpreted via a dynamic correlation length, show a clear indication of the transition to  $B\mu E$ , and the location of the transition is not entirely consistent with previous suggestions for o/w/s systems. The remainder of the paper is organized as follows. First we review some of the experiments on polymeric and o/w/s microemulsions, and recall the predictions of the Teubner–Strey model.<sup>5</sup> Following Sec. III, we present our results on two systems. The emphasis is on the structure factor obtained by SANS, and on the dynamic correlation length obtained by DLS. The combination of these results leads to the conclusion that the transition to the  $B\mu E$  phase is best indicated by the temperature dependence of the dynamic correlation length, and we propose that it is the homopolymer/homopolymer Lifshitz line that comes closest to marking this transition. In the final sections we analyze the structure of the interfaces, and systematic deviations from the Teubner–Strey description, in more detail.

## II. BACKGROUND: BICONTINUOUS MICROEMULSIONS

Bicontinuous microemulsion phases ( $B\mu E$ ) are by now well established in o/w/s systems, for both ionic and non-ionic surfactants and in the presence or absence of fourth components such as salt or cosurfactants.<sup>1,2,4,6</sup> They are characterized by very small interfacial tensions and nearly zero spontaneous curvature. They tend to exist over a rather narrow range of temperature for a given composition, due to the asymmetric temperature dependence of the o/s and w/s interactions. More recently, the analogous  $B\mu E$  phase has been identified in four ternary polymer blends, containing homopolymers A and B and an AB block copolymer.<sup>7–10</sup> In all four cases the systems were carefully constructed to be symmetric in composition and to have experimentally accessible phase transition temperatures. In particular, the degrees of polymerization  $N_A \approx N_B$ ,  $N_{AB} \approx 5N_A$  were chosen to place the critical temperature of the binary blend and the order–disorder transition of the pure copolymer in a convenient range, and the copolymers were roughly symmetric (volume fraction  $f_A \approx 0.5$ ). Under these conditions the phase diagram near the isopleth (the temperature/copolymer concentration plane with homopolymer volume fractions  $\phi_A = \phi_B$ ) has the general form illustrated in Fig. 1. There are three broad regimes of behavior. At high temperatures a molecularly mixed, disordered fluid exists for all copolymer concentrations. At low temperatures this gives way to an ordered, lamellar phase for copolymer concentrations above 15%–20%, and to phase separation (two or three phases coexisting) at low copolymer concentrations (less than 10%). In between the lamellar phase and the phase-separated regime there is a narrow channel of a disordered phase that has been characterized as  $B\mu E$ .<sup>7,8</sup>

Mean-field theory often provides an excellent starting point for describing the thermodynamics of polymer mixtures, and this is the case for ternary blends. For the ternary system just described, mean-field theory anticipates all of the features of Fig. 1 except for the  $B\mu E$ .<sup>11–15</sup> Instead, the line of order–disorder transitions meets the line of second-order critical points at an isotropic Lifshitz point,<sup>11,12</sup> and the

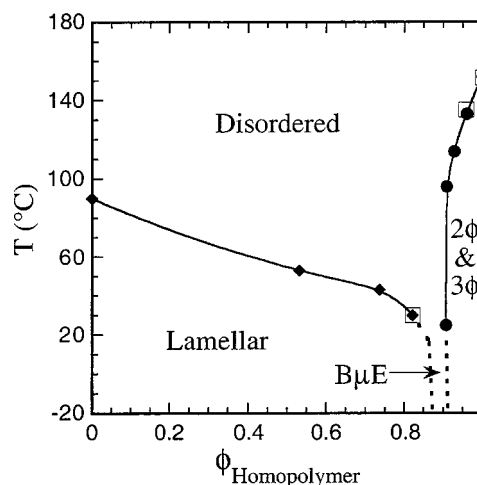


FIG. 1. Phase diagram along the isopleth for the PEE/PDMS/PEE-PDMS ternary system (Ref. 10).

lamellar and phase-separated regions meet at an unbinding transition. Fluctuations, however, are expected to destroy the Lifshitz point, and the experimental appearance of the  $B\mu E$  may be qualitatively understood in this light.<sup>14,16,17</sup> A first step toward incorporation of fluctuation effects into the ternary phase prism has been reported by Kielhorn and Muthukumar.<sup>14</sup> However, a full theoretical description of the transition from disordered fluid to  $B\mu E$  is not yet available. Consequently, it is not immediately apparent what experimental signature(s) are most useful or appropriate to mark this boundary. To pursue this issue, it is instructive to recall some of the recent progress in o/w/s systems, and in particular the Teubner–Strey description.<sup>5</sup>

Teubner and Strey presented a phenomenological theory for the structure factor of a  $B\mu E$  by an expansion of the Landau free energy to second order in the order parameter,  $\Psi$ , the concentration difference between components; only even order terms contribute due to symmetry.<sup>5</sup> Because of the microdomain structure, gradient terms must be included. The spontaneous creation of interface requires a negative coefficient in the gradient squared term, and stability requires a positive higher order term. The simplest free energy density for this system is thus

$$F = a_2 \Psi^2 + c_1 (\nabla \Psi)^2 + c_2 (\nabla^2 \Psi)^2. \quad (1)$$

This yields for the scattering intensity

$$I(q) = \frac{1}{a_2 + c_1 q^2 + c_2 q^4}, \quad (2)$$

where the proportionality constant is absorbed into the free energy coefficients. When  $c_1^2/(4a_2c_2) < 1$ , the inverse Fourier transform of  $I(q)$  yields the following correlation function:

$$g(r) = \frac{d}{2\pi r} \exp[-r/\xi_{TS}] \sin\left(\frac{2\pi r}{d}\right) \quad (3)$$

where the domain periodicity,  $d$ , and the correlation length,  $\xi_{TS}$ , are the two relevant static length scales:

$$\xi_{TS} = \left[ \frac{1}{2} \left( \frac{a_2}{c_2} \right)^2 + \frac{1}{4} \frac{c_1}{c_2} \right]^{-1/2} \quad (4)$$

and

$$d = 2\pi \left[ \frac{1}{2} \left( \frac{a_2}{c_2} \right)^{1/2} - \frac{1}{4} \frac{c_1}{c_2} \right]^{-1/2}. \quad (5)$$

The functional form of  $g(r)$  reflects two properties of B $\mu$ E: alternating component-rich domains of average size  $d/2$ , described by the sinusoidal term, and short-range order among the domains over the correlation length  $\xi_{TS}$ , described by the exponential term. Thus the three fitting coefficients,  $a_2$ ,  $c_1$ , and  $c_2$ , can be reformulated as the physically more transparent values,  $\xi_{TS}$ ,  $d$ , and the susceptibility  $I(0)$ , which is inversely proportional to  $a_2$ .

Strey *et al.*<sup>18–20</sup> have further classified the differently structured fluids in the disordered phase of the o/w/s system by defining the amphiphilicity factor,  $f_a \equiv c_1 / (4a_2c_2)^{1/2}$ , and extending the Teubner–Strey model over all ranges of amphiphilicity. (We note that here  $f_a$  is defined with respect to the water/water structure function.) For strong amphiphilicity with  $f_a < -1$ , the microemulsion phase is unstable with respect to the lamellar phase. With slightly less amphiphilicity,  $-1 < f_a < 0$ , a strongly structured, “good” microemulsion results (note that “amphiphilicity” increases as  $f_a$  decreases). One distinguishing characteristic of a “good” microemulsion is the tendency to create interface due to a vanishing or negative microscopic surface tension. This corresponds to a negative value of  $c_1$  (and thus negative  $f_a$ ). This leads to a strong correlation between the interfaces, which dominates the scattering and produces a peak at a finite  $q^*$ . A further decrease in amphiphilicity,  $0 < f_a < 1$ , results in a “poor” microemulsion. Here, the correlation function  $g(r)$  is still oscillatory, but interfacial correlations no longer dominate the scattering and the structure factor peak occurs at zero wave vector. Finally, for  $f_a > 1$ , the fluid is unstructured and  $g(r)$  is no longer oscillatory. The boundaries between these classifications do not correspond to thermodynamic transitions, but are simply demarcations between differently structured fluids. The (water/water) Lifshitz line (corresponding to the structure function usually measured by SANS) is defined by  $c_1 = f_1 = 0$ , and marks the boundary between “good” and “poor” microemulsions. The disorder line at  $f_a = 1$  signifies the transition from correlated to non-correlated interfaces. These lines can be defined equivalently via the two static length scales  $\xi_{TS}$  and  $d$  introduced previously: At the Lifshitz line,  $2\pi\xi_{TS}/d = 1$ , and at the disorder line,  $2\pi\xi_{TS}/d = 0$ .

Schubert *et al.*<sup>19</sup> investigated the relationship between the microemulsion transition and the previously defined lines in water/*n*-alkane/ $C_{12}E_j$  nonionic surfactant mixtures. In particular, they located the wetting/nonwetting transition, where in a three-phase mixture the microemulsion phase either wets, or does not wet, the oil-rich and water-rich phases. Theoretical work had suggested that this wetting transition was associated with the disorder line, and may be associated with a change in the fluid structure, and thus represent the primary demarcation between microemulsions and less structured fluids.<sup>21</sup> Experimentally, however, this transition was

found to occur near  $f_a \approx -0.33$ , i.e., closer to the Lifshitz line than to the disorder line. On this basis, Schubert *et al.* did not suggest that a particular line was the dominant microemulsion transition, but rather that these lines just separated different strengths of microemulsion on the approach toward the lamellar phase.<sup>19</sup>

It is clearly of interest, therefore, to consider polymeric B $\mu$ Es in this context, and to see whether similar conclusions can be drawn. In particular, how does the appearance of the B $\mu$ E in the polymer case correlate with the amphiphilicity factor, and the disorder and Lifshitz lines? It is important to note that in a ternary system there should be multiple Lifshitz and disorder lines in principle.<sup>12</sup> In the o/w/s system SANS typically distinguishes the deuterated water from the other components and the measured  $I(q)$  corresponds to the water/water structure function. Further Lifshitz lines are determined by the (partial) structure functions corresponding to the oil structure and to the structure of each component of the amphiphile; incompressibility reduces the number of independent structure functions by one. The disorder lines corresponding to the different structure functions should be degenerate.<sup>12</sup> In the polymer systems used here the A and B homopolymers have the same isotopic compositions as the corresponding blocks in the copolymer, and therefore SANS reflects the total monomer A/monomer B structure function.

### III. EXPERIMENT

#### A. Materials

Two blend systems were studied. One, designated “EED,” comprises polyethylene (PEE), polydimethylsiloxane (PDMS), and the corresponding symmetric block copolymer PEE–PDMS. All three components were synthesized anionically using standard procedures, producing low polydispersity samples ( $M_w/M_n < 1.1$ ), as previously described.<sup>8</sup> The PEE was prepared by first synthesizing polybutadiene (90% 1,2 and 10% 1,4 addition), followed by catalytic deuteration. The number average molecular weights,  $M_n$ , as measured by NMR are 1770 for PEE, 2130 for PDMS, and 10 400 for PEE–PDMS. The composition of the diblock is 48% PEE by volume (calculated from the weight fraction assuming homopolymer densities of 0.883 g/mL for PEE and 0.954 g/mL for PDMS, respectively<sup>8</sup>). Each mixture contains equal volumes of PEE and PDMS homopolymer, and they are denoted according to the volume percent of copolymer: 0%, 4.2%, 7.1%, 9.2%, 10%, 12%, 15%, and 26.4%. We note that these mixtures deviate slightly from the critical compositions. The other system, designated “PO,” comprises poly(ethylenepropylene) (PEP), polyethyleneoxide (PEO), and the corresponding symmetric block copolymer PEP–PEO. The PEP is actually squalane (Aldrich), a saturated hydrocarbon with six pendant methyl groups along the backbone, having a molecular weight of 423 g/mol. The PEO was purchased from Aldrich, and has  $M_n = 500$  g/mol with  $M_w/M_n = 1.1$ . The purification of PEP and PEO was previously described.<sup>9</sup> The PEP–PEO copolymer was synthesized according to the procedure of Hillmyer and Bates,<sup>22</sup> as previously described.<sup>9</sup> The characteristics are  $M_n = 3000$ ,  $M_w/M_n = 1.2\%$  and 50% PEP by volume (cal-

culated from the weight fraction assuming densities of 0.81 and 1.07 g/mL for PEP and PEO, respectively<sup>9</sup>). The two PO blends examined contained a 60:40 volume ratio of PEP to PEO, and either 10% or 11% copolymer by volume.

## B. Rheology

Dynamic shear measurements on the 10% EED and 11% PO blends were made on a Rheometrics DSR rheometer. The sample chamber was maintained under nitrogen and the temperature controlled to within  $\pm 1^\circ$ . Stress sweeps were performed to establish that the measurements were made in the linear viscoelastic regime. Frequency sweeps from 100 to 0.01 Hz were performed from 25 to 150  $^\circ\text{C}$  for EED, and the dynamic viscosity,  $\eta'$ , extrapolated to zero frequency (most measurements were constant over this frequency range). The shear viscosity thus obtained was fit to the Williams–Landel–Ferry (WLF) equation.<sup>23</sup> Values for the other mixtures were then estimated by (i) assuming that  $\eta \sim N$  using the average  $N$  for each mixture (i.e., Rouse dynamics<sup>23</sup>), and (ii) using the same WLF coefficients as determined for the 10% mixture. For the 11% PO blend stress sweeps were performed from 100 to 160  $^\circ\text{C}$  with shear rates from 1 to 100  $\text{s}^{-1}$ ; the viscosities were then extrapolated to zero shear rate. The viscosity of the 10% blend was estimated via the same Rouse assumption.

## C. Neutron scattering

SANS measurements were performed on the 30 m Exxon/Minnesota/NIST instrument at NIST (NG-7). Samples were contained in cells fashioned from two 1/16-in.-thick quartz disks sealed around the edges. Measurements were taken with an incident wavelength,  $\lambda$ , of 6 Å (EED) or 7 Å (PO), a wavelength spread,  $\Delta\lambda/\lambda$  of 11%, and sample-to-detector distances from 7 to 15 m. Intensities from a two-dimensional detector were azimuthally averaged, corrected for background, transmission, empty cell and incoherent scattering, and finally converted to absolute intensity,  $I(q)$ , where  $q = (4\pi/\lambda)\sin(\theta/2)$  is the scattering vector, using appropriate standards.

## D. Dynamic light scattering

DLS measurements were taken using either an Ar<sup>+</sup> (488.0 nm) or HeNe laser (632.8 nm), and either a Brookhaven Instruments BI-9000 or an ALV-5000 correlator. EED mixtures were made by dissolving each polymer in pentane and filtering through a 0.45  $\mu\text{m}$  filter into 5-mm-o.d. glass tubes. After evaporating the pentane, the glass tubes were vacuum sealed. PO samples were prepared by similar methods using methylene chloride as solvent. The sample was immersed in a bath of index-matching fluid (silicone oil) with temperature controlled to  $\pm 0.1^\circ\text{C}$ . Measurements were taken at angles from 30 $^\circ$  to 150 $^\circ$ , with the majority at 90 $^\circ$ , for temperatures from 0 to 180  $^\circ\text{C}$  for EED and from 60 to 160  $^\circ\text{C}$  for PO. Autocorrelation functions of the scattered light intensity,  $g^{(2)}(q, t)$ , were analyzed either by a nonlinear regularized inverse Laplace transformation algorithm, REPES,<sup>24</sup> giving a distribution of relaxation rates,  $\Gamma$ , or by fitting to a single exponential decay. In the disordered

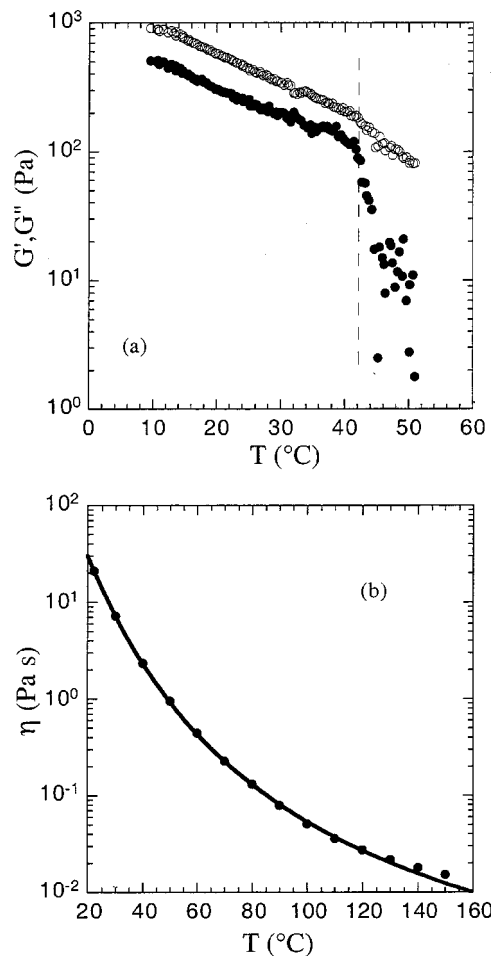


FIG. 2. Rheological measurements on EED blends. (a) Dynamic shear moduli as a function of temperature for the 26.4% mixture. The order–disorder transition is indicated by the dashed line. (b) Zero-shear rate viscosity as a function of temperature for the 10% mixture. The sample is disordered throughout, and is a bicontinuous microemulsion at low temperatures.

one-phase mixtures, most correlation functions were well described by a single exponential relaxation, but evidence of multiple modes was found in the bicontinuous microemulsions. We define a dynamic correlation length,  $\xi_d$ , by invoking the Kawasaki–Stokes equation:

$$\Gamma = Dq^2 = \frac{k_B T}{6\pi\eta\xi_d} q^2, \quad (6)$$

where  $\eta$  is the zero shear viscosity and  $D$  is the measured mutual diffusion coefficient (from plots of  $\Gamma$  vs  $q^2$ ).

## IV. RESULTS AND DISCUSSION

### A. Rheology

Rheology is a useful tool for locating phase transitions or other macroscopic structural changes in polymer materials. In Fig. 2(a), the dynamic shear moduli ( $G'$  and  $G''$ ) for the EED blend containing 26.4% copolymer measured at a fixed frequency of 40 rad/s are plotted as a function of temperature. An order–disorder transition (ODT) occurs where the behavior of the moduli abruptly change (the dotted line in Fig. 2). The ODT is a first-order phase transition from the



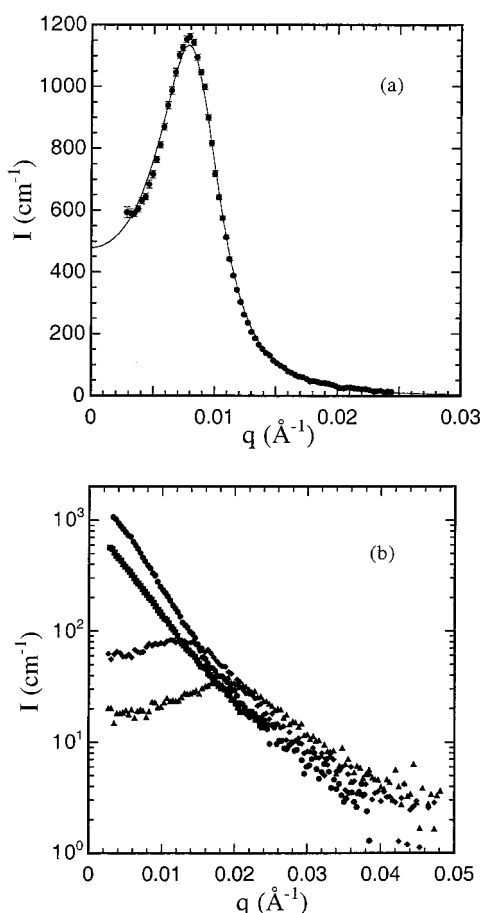


FIG. 3. SANS intensity as a function of scattering vector,  $q$ , for EED blends: (a) 10% mixture at room temperature; the line is a fit to the Teubner–Strey model, (b) measurements at 90 °C for the 9.2% (●), 10% (■), 12% (◆), and 15% (▲) samples.

disordered phase at high temperature to the lamellar phase at low temperature (the anticipated narrow coexistence region is not resolved). The disordered phase exhibits liquidlike rheological properties:  $G''$  is much larger than  $G'$ , and  $G'$  decreases rapidly with increasing temperature. The lamellar phase is more solidlike (albeit a soft solid):  $G' \approx G''$ , and the moduli vary gradually with temperature.

In contrast, no phase transition is observed in the EED sample with 10% copolymer, which was previously shown to exhibit B $\mu$ E behavior.<sup>8,10</sup> The temperature dependence of the zero shear viscosity of this 10% blend is shown in Fig. 2(b), from deep in the microemulsion channel at room temperature to well above the microemulsion regime at high temperature. The sample consistently exhibits terminal flow behavior over the entire temperature range examined:  $G''$  is much larger than  $G'$ , and is proportional to frequency. In addition, the temperature dependence fits well to the WLF equation. Thus, although both lamellar (not shown) and B $\mu$ E blends can exhibit a strong scattering peak, their rheological properties are quite distinct.

## B. Neutron scattering

Figure 3 displays typical SANS data for EED mixtures. The structure function  $S(q)$  is plotted as the scattering inten-

sity,  $I(q)$  (in absolute units,  $\text{cm}^{-1}$ ) versus scattering wave vector,  $q$ . Recall that in this case,  $I(q)$  corresponds to the total monomer structure function, in contrast to the o/w/s system. Figure 3(a) shows the scattering from the 10% blend at 25 °C, deep in the microemulsion channel. Characteristic microemulsion behavior is seen here, with one broad peak at low  $q$ , and with  $I(q)$  falling off as  $q^{-4}$  at higher  $q$ . The curve in Fig. 3(a) is a fit to the Teubner–Strey function [Eq. (2)], which describes the data well. Figure 3(b) compares  $I(q)$  for four samples, 9.2%, 10%, 12%, and 15%, taken at 90 °C. At this temperature, a range of behavior is seen. Although the large  $q$  scattering ( $q > 0.02 \text{ \AA}^{-1}$ ) is similar, the low  $q$  behavior ( $q < 0.02 \text{ \AA}^{-1}$ ) is clearly different (note the logarithmic intensity scale). For the two blends with higher block copolymer concentrations, a peak at finite  $q$  is evident, whereas for the two lower concentration samples the intensity continues to increase with decreasing  $q$ , signifying a different structure. Analogous SANS pattern for the PO system were presented previously.<sup>9</sup>

The Teubner–Strey fitting parameters  $a_2$ ,  $c_1$ , and  $c_2$  for EED blends are shown in Figs. 4(a) and 4(b), respectively, from room temperature up to 195 °C, to distinguish these four mixtures. The coefficient  $a_2$  varies by three orders of magnitude over this temperature range, and is plotted semi-logarithmically in Fig. 4(a). The 9.2% and 10% samples show a minimum around 90 °C, whereas the 12% and 15% samples increase monotonically with increasing temperature. The parameter  $c_1$ , plotted in Fig. 4(b), is most closely related to the interfacial tension. The two lower block copolymer concentration samples have  $c_1 < 0$  at low temperatures, and cross the Lifshitz line ( $c_1 = 0$ ) around 80 °C, with  $c_1 > 0$  at higher temperatures. In contrast, neither of the higher concentration samples cross the Lifshitz line, but remain in the  $c_1 < 0$  regime. Since the block copolymer acts as a surfactant, increasing the block copolymer concentration should decrease  $c_1$ , as observed. The behavior of  $c_2$ , plotted in Fig. 4(c), is similar for all four samples, decreasing monotonically with increasing temperature.

In Fig. 5 the amphiphilicity factor as calculated from the energy coefficients is plotted as a function of temperature, for the same four samples. The two lower block copolymer concentration samples access a broad range of behavior, crossing both the Lifshitz and the disorder lines. Deep in the microemulsion channel, each mixture is a “good” microemulsion, i.e., as characterized by a large negative  $f_a$ . As temperatures increases the Lifshitz line is crossed at 72 °C for the 10% sample and 82 °C for the 9.2% sample, thereby transforming to “poor” microemulsions. Upon further increases in temperature, both cross the disorder line, at 85 °C for the 10% sample and 92 °C for the 9.2% sample. With further increase in temperature for the 9.2% blend,  $f_a$  peaks, decreases, crosses below the disorder line at 113 °C, and asymptotes to a value of about 0.4 at high temperature. The decreasing trend is due to a significant increase in  $a_2$  rather than a decrease in  $c_1$  ( $c_1$  is increasing throughout this temperature range) and thus  $f_a$  is not approaching the Lifshitz line at this temperature range. This result is in possible conflict with the results of Schwahn *et al.*, who report a second crossing of the Lifshitz line at high temperature in the same

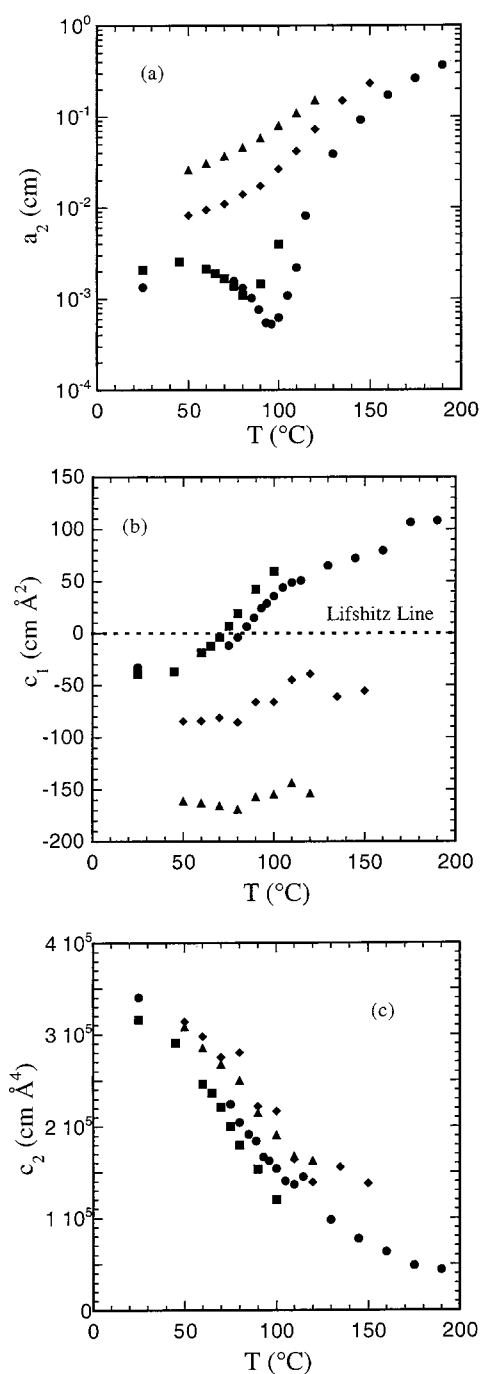


FIG. 4. Coefficients of the Teubner–Strey fits: (a)  $a_2$ , (b)  $c_1$ , and (c)  $c_2$  plotted as a function of temperature for the 9.2% (●), 10% (■), 12% (◆), and 15% (▲) samples.

system.<sup>16,17</sup> The higher concentration samples, in contrast, remain in the “good” microemulsion regime throughout the measured temperature range, with a steady increase in  $f_a$  with increasing temperature. This increase is also mainly due to  $a_2$ . In general the approach to the Lifshitz line with temperature is dominated by the interfacial tension ( $c_1$ ), whereas the approach to the disorder line is dominated by the susceptibility ( $a_2$ ).

In Figs. 6(a)–6(c) we show the static length scales,  $\xi_{TS}$  and  $d/2$ , and the susceptibility,  $I(q=0)$ , respectively, as functions of temperature. The correlation length  $\xi_{TS}$  appears

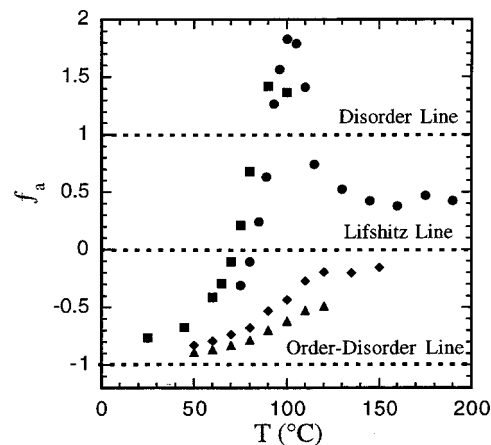


FIG. 5. Amphiphilicity factor from SANS measurements as a function of temperature for the 9.2% (●), 10% (■), 12% (◆), and 15% (▲) samples.

to have almost no concentration dependence, but depends strongly on temperature;  $\xi_{TS}$  is unaffected by which region of microemulsion behavior the mixture is in (i.e.,  $f_a$ ). Apparently,  $\xi_{TS}$  is determined mainly by the specific surfactant through  $c_2$ , rather than by the fluid structure. In other words because  $c_2$  reflects mainly the large  $q$  behavior (see the following), it is most closely related to the structure of the interfaces. Thus the monotonic increase of  $\xi_{TS}$  with decreasing temperature indicates a progressive “stiffening” of the interfaces. This conclusion will be supported by further analysis in Sec. IV E.

The domain size,  $d/2$ , which is defined only below the disorder line, decreases slightly with increasing temperature below the Lifshitz line, but diverges as the disorder line is approached [evident in the 9.2% and 10% samples, Fig. 6(b)]. The divergence heralds the falling apart of the  $B\mu E$ , whereas the slight increase with decreasing temperature below 50 °C presumably is due to increased copolymer chain stretching. In contrast,  $\xi_{TS}$  is insensitive to either the disorder line or the Lifshitz line. Also in contrast to  $\xi_{TS}$ , the domain size decreases significantly with increasing block copolymer concentration, as expected; the concentration of block copolymer should determine the amount of interface the fluid can support. Similarly,  $\xi_{TS}/d$  increases with increasing copolymer concentration, as expected from the Teubner–Strey model, and this increase is another characteristic common to surfactant systems. Deep in the  $B\mu E$  channel, in the “good” microemulsion regime, the domain size is well established and largely independent of the magnitude of  $f_a$ .

The susceptibility [Fig. 6(c)] also shows a significant difference between the lower and higher block copolymer concentration samples. At the lower concentrations, where the mixtures access the full range of amphiphilicity,  $I(0)$  peaks at 95 °C for the 9.2% sample, and at 80 °C for the 10% sample. For the higher concentration samples,  $I(0)$  decreases continuously with increasing temperature. In the “good” microemulsion regime,  $I(0)$  increases with decreasing amphiphilicity ( $f_a$  becoming more positive) for the 9.2% and 10% samples, whereas the opposite trend occurs in the “good” microemulsion regime for the higher concentration samples. In the samples which cross the Lifshitz line with

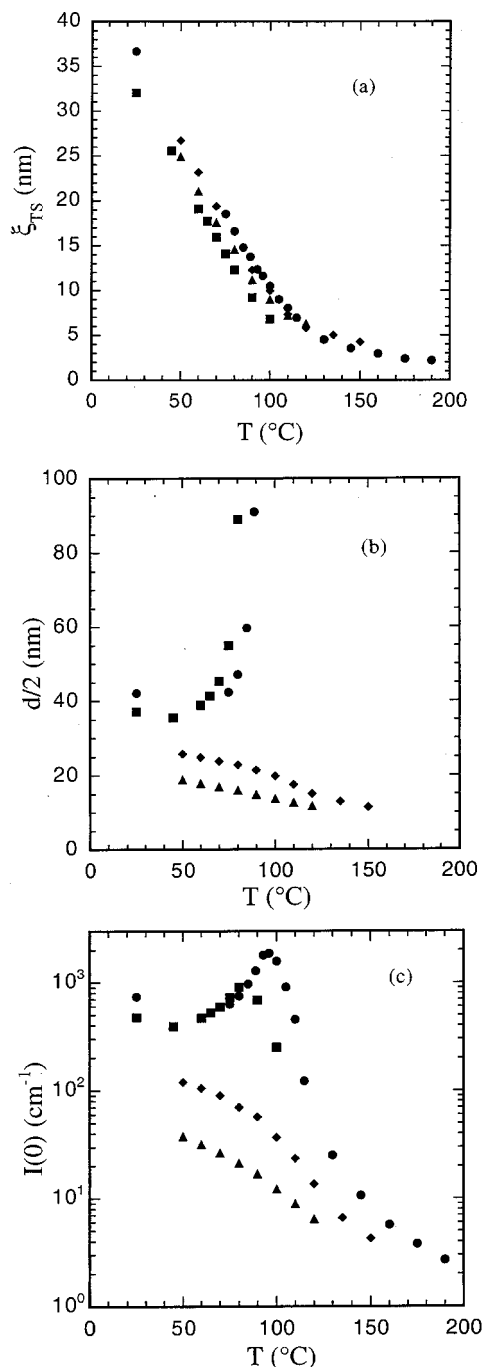


FIG. 6. Teubner–Strey parameters: (a) correlation length, (b) domain size, and (c) susceptibility as a function of temperature for the 9.2% (●), 10% (■), 12% (◆), and 15% (▲) samples.

temperature there is a corresponding peak in  $I(0)$ , whereas those that do not cross the Lifshitz line do not have this peak.

### C. Dynamic light scattering

Dynamic light scattering is often used to probe the dynamics of concentration fluctuations in complex fluid mixtures. In particular, the order parameter fluctuations in binary polymer blends in the one-phase region near the critical point have been studied in some detail.<sup>25–28</sup> The experimental intensity correlation functions are well described by a single exponential decay, and the decay rate interpreted via the

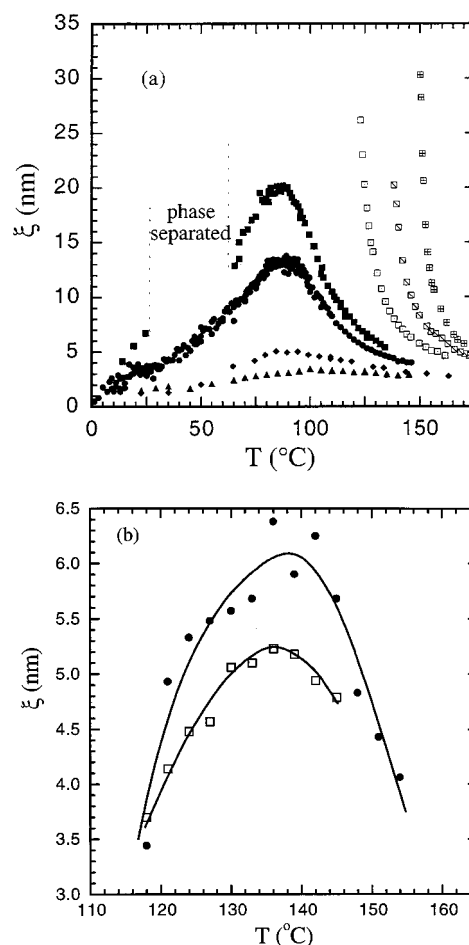


FIG. 7. Dynamic correlation length from DLS as a function of temperature for (a) the 0% (□), 4% (□), 7.1% (□), 9.2% (■), 10% (●), 12% (◆), and 15% (▲) EED samples and (b) 10% (●) and 11% (□) PO samples. The 9.2% EED mixture has a phase-separated window surrounded by two microemulsion regions at low temperature. The curves in (b) are guides to the eye.

Kawasaki–Stokes relation [Eq. (6)]. The resulting dynamic correlation length,  $\xi_d$ , diverges as the spinodal temperature  $T_s$  is approached. The nature of the divergence shows a broad crossover from mean-field scaling far above the stability limit ( $\xi_d \sim (1/T_s - 1/T)^{-\nu}$ , with  $\nu=0.5$ ) to Ising scaling ( $\nu=0.63$ ) near to  $T_s$ . The behavior of the dynamic correlation length parallels that of the static correlation length,  $\xi_s$ , obtained from the (Ornstein–Zernicke-type) structure factor. We have previously shown that the PEE/PDMS binary blend shows behavior that is consistent with other, more detailed reports.<sup>10</sup>

With the addition of block copolymer to the binary blend more complicated behavior may be expected. However, for the relatively modest amounts of copolymer employed here, we assume that the principal dynamic mode still reflects dynamics of A/B homopolymer concentration fluctuations, as mediated by the presence of copolymer. Figure 7(a) shows  $\xi_d$  vs  $T$  for the 0%, 4.2%, 7.1%, 9.2%, 10%, 12%, and 15% EED samples over the accessible range of temperature. For the lowest three concentrations  $\xi_d$  diverges as the phase boundary is approached. In these mixtures the correlation functions were well described by single exponential decays. As shown previously, the critical exponent  $\nu$  apparently in-

creases in magnitude with added copolymer from the Ising result in the binary blend;<sup>10</sup> this is consistent with the extensive SANS results of Schwahn *et al.*<sup>16,17</sup> on the same system. Upon entering the microemulsion channel, however, the behavior of  $\xi_d$  changes abruptly. For the four higher concentrations  $\xi_d$  exhibits a clear maximum before decreasing as temperature is further decreased. (The gap in the data for the 9.2% sample represents a “reentrant” region of phase separation, see Fig. 1.) This maximum is arguably the most distinctive experimental indication of the formation of a bicontinuous microemulsion. It occurs because the dynamics of spontaneous concentration fluctuations are very sensitive to the underlying fluid structure. On cooling from the fully disordered phase, the dynamic correlation length increases due to the longer ranged, larger amplitude fluctuations, reminiscent of critical slowing down. However, the formation of the microemulsion arrests the divergence. Similarly, on heating from the fully formed microemulsion, the loosening of the interfaces inferred from the parameters in Figs. 4 and 6 also retards the relaxation of concentration fluctuations, leading to an increase in  $\xi_d$ . The two competing trends result in the peak in  $\xi_d$ ; the strong peak in the 9.2% and 10% samples is also consistent with the corresponding peaks in  $I(0)$ . Importantly, the universality of the peak in  $\xi_d$  is demonstrated in Fig. 7(b), where data for the two PO blends are shown. Although in this case the data are less plentiful, the existence of the peaks is clearly established.

In many mixtures, such as binary polymer blends and semidilute polymer solutions,  $\xi_d$  follows closely the behavior of the static correlation length. This is not the case here; the behavior of  $\xi_d$ , in contrast to  $\xi_{TS}$ , changes dramatically between the high and low temperature regions of the disordered phase. In all four microemulsion-forming EED samples,  $\xi_d$  is small at high temperatures, grows as temperature decreases, peaks around 90 °C, and decreases with further decrease in temperature. The height of the peak decreases with increasing copolymer concentration, from ~20 nm for the 9.2% mixture to 3.5 nm for the 15% mixture, but the peak temperature remains approximately the same. This should be contrasted with the monotonic temperature dependence of  $\xi_{TS}$  in Fig. 6(a). The same trends in  $\xi_d$  are seen for the two PO blends in Fig. 7(b); the peak height decreases with increasing copolymer concentration, but the peak position remains roughly independent of temperature (135–140 °C).

In addition to the peak in  $\xi_d$ , the transition to B $\mu$ E behavior has two other signatures in the DLS properties. As noted previously, the correlation functions in the microemulsion channel are not strictly single exponential decays, in contrast to the higher temperature correlation functions.<sup>10</sup> Specifically, they contain one or two low amplitude, faster modes in addition to the main mode associated with  $\xi_d$ . These modes were tentatively attributed to copolymer or interfacial undulation dynamics,<sup>10</sup> but further experiments to characterize their origin more fully are beyond the scope of this work. The other, more conclusive effect is that the main mode does not behave in a strictly diffusive manner in the microemulsion regime. The additional  $q$  dependence is a result of the  $q$  dependence of the mutual diffusion coefficient. For example, the Teubner–Strey model predicts that the mi-

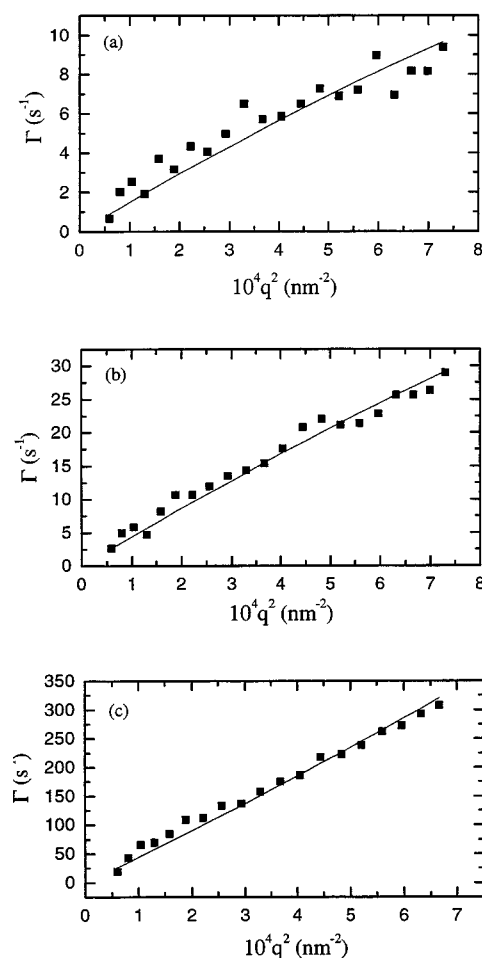


FIG. 8. Angular dependence of the decay rate  $\Gamma$  (corresponding to the primary mode) for the 10% EED sample at (a) 25 °C, (b) 45 °C, (c) 100 °C. The solid lines are obtained using the Teubner–Strey parameters calculated from SANS data.

croemulsion structure will affect the collective diffusion constant by<sup>5</sup>

$$D(q) = D(0) \left( 1 + \frac{c_1}{a_2} q^2 + \frac{c_2}{a_2} q^4 \dots \right), \quad (7)$$

where the coefficients involve the same parameters as the structure factor SANS fit. In Figs. 8(a)–8(c), we plot  $\Gamma$  of the main mode as a function of  $q^2$  for the 10% EED mixture at three different temperatures (100, 45, and 25 °C). The former lies above the maximum in  $\xi_d$ , but the latter two fall in the B $\mu$ E regime. For  $q$ -independent diffusive dynamics, the data should follow a straight line, but the lower temperature results clearly have an additional  $q$  dependence. The smooth curves correspond to Eq. (7), using the values of the three Teubner–Strey parameters extracted from fits to the SANS data. The agreement is quite reasonable, although for the lowest temperature the DLS  $q$  dependence appears to be slightly stronger than anticipated on the basis of the structure factor fit. We therefore conclude that the DLS results develop an additional  $q$  dependence in accordance with the Teubner–Strey model only in the temperature range below the maximum in  $\xi_d$ , thereby supporting the inference that this peak is a good indicator of the transition to B $\mu$ E. In



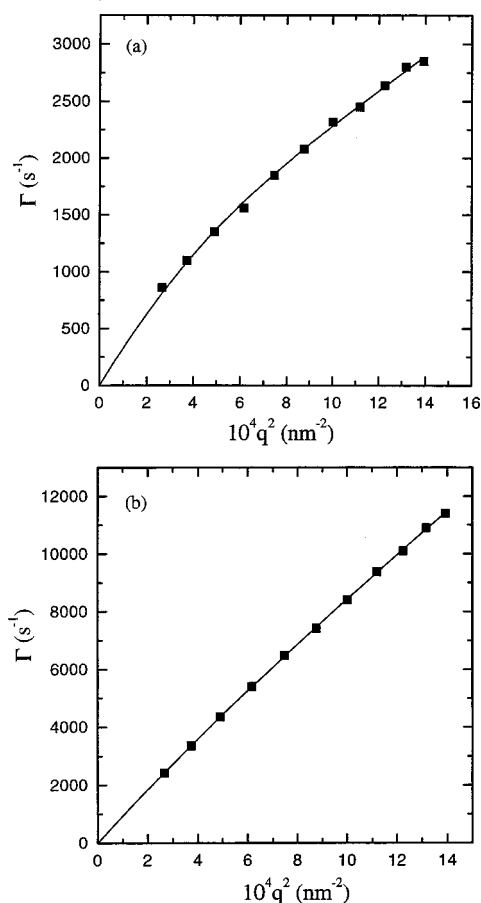


FIG. 9. Angular dependence of the decay rate  $\Gamma$  (corresponding to the primary mode) for the 11% PO sample at (a) 117 °C, (b) 145 °C. The solid lines are polynomial fits from which the amphiphilicity factor is calculated.

Figs. 9(a) and 9(b) we show the same DLS quantity for the 11% PO system at 117 and 145 °C, respectively. However, in this case the smooth curves are direct fits to the data using Eq. (7). There is considerably more curvature in the plot at the lower temperature, consistent with the well-developed B $\mu$ E structure. The resulting parameter values are then employed to calculate the amphiphilicity factor,  $f_a$ , as shown versus temperature in Fig. 10. Three values of  $f_a$  obtained

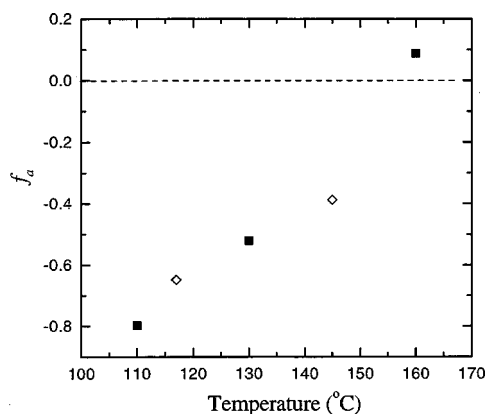


FIG. 10. Amphiphilicity factor as a function of temperature for the 11% PO sample from both SANS (■) and DLS (◇).

from SANS are also shown, and the two techniques gives satisfactory agreement.

#### D. Revised phase diagrams

Figures 11(a) and 11(c) show modified phase diagrams (temperature versus copolymer concentration) for EED and PO blends, respectively. The important new features for EED, relative to the previous version,<sup>8,10</sup> are the addition of the disorder line, the total monomer Lifshitz line, and points denoting the maxima in the dynamic correlation length. The two lines are drawn based on the amphiphilicity factor. For example, the 12% and 15% samples are below the Lifshitz line ( $f_a < 0$ ) for all measured temperatures; whereas the 10% and 9.2% are above the Lifshitz line at high temperatures. The Lifshitz line is thus nearly temperature independent (i.e., vertical) for concentrations between 10% and 12%. Similarly, the 7.1% samples is above the disorder line as determined by SANS for all measured temperatures, whereas the 9.2% sample is below the disorder line at high temperatures. Both lines are thus nearly temperature independent except in a small region around the mean-field-predicted Lifshitz point. It is important to note that, at least in the polymeric case, neither the disorder line nor the total monomer Lifshitz line is sufficient to demarcate the different microemulsion phases. For example, a one-component disordered block copolymer at high temperatures would be defined as a microemulsion because it lies beyond the disorder line (the disorder lines should be the same for the different structure functions<sup>12</sup>). This structure clearly lies outside of the definition of microemulsion, however, and the scattering peak in disordered block copolymers is due to the correlation hole caused by the connectivity of the chains, rather than any particular microemulsion structure. In contrast to previous o/w/s studies,<sup>18,19,21</sup> we can thus rule out the disorder line as a reliable demarcation line even for weak microemulsion structures. Instead, this line designates only increased amphiphilicity due to, e.g., higher surfactant concentration or lower temperature. The same reasoning implies that the total monomer Lifshitz line is also not a precise or particularly useful microemulsion demarcation, and therefore neither are all Lifshitz lines demarcations for microemulsion phases.

In contrast, the  $\xi_d$  peak position line is nearly horizontal, and thus uncorrelated with the SANS-measured disorder or total monomer Lifshitz lines. If  $\xi_d$  were related to the total monomer dynamics, we might expect the peak to correspond to the total monomer Lifshitz line. However, because the main decay mode changes continuously when block copolymer is added to the binary blend, DLS appears to instead probe homopolymer/homopolymer (h/h) dynamics. (Additional small amplitude decay modes, which are probably associated with block copolymer and/or interface dynamics, do appear at lower temperatures as noted previously.) Thus we propose that the peak in  $\xi_d$  is correlated with the h/h Lifshitz line, and that therefore this feature may be the most useful demarcation of B $\mu$ E behavior. This proposed correlation cannot be established without additional SANS measurements on samples with different deuterium labeling. However, the hypothesis draws qualitative support from mean-field theory on a similar ternary system.<sup>12</sup> We present a

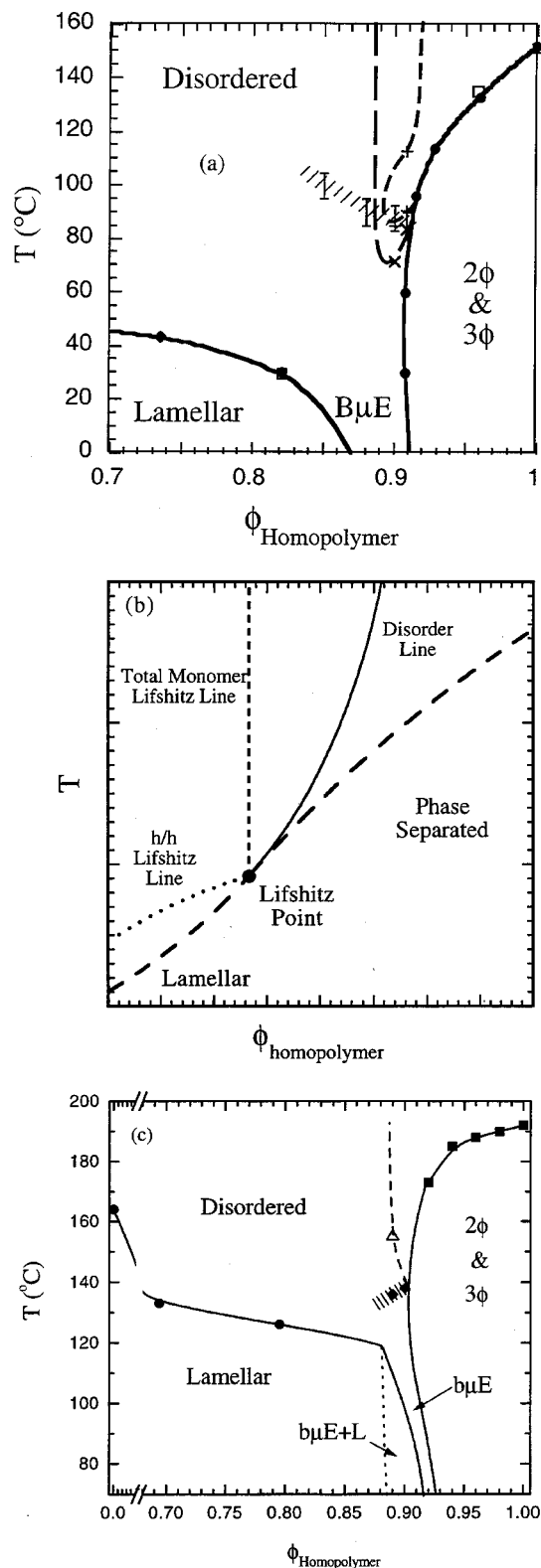


FIG. 11. Phase diagrams along an isopleth including lines distinguishing differently structured disordered phases as measured by SANS and DLS. (a) Experimental phase diagram for the EED system: The shorter-dashed line is the disorder line and the longer-dashed line is the total monomer Lifshitz line. The error bars and hatched region correspond to the dynamic correlation length peak. (b) Theoretical mean-field phase diagram: an isotropic Lifshitz point exists at the intersection of the line of critical points, line of order-disorder transitions, and the disorder line and Lifshitz lines (Ref. 12). (c) Experimental diagram for the PO system (Ref. 9). The dashed line is the total monomer Lifshitz line, and the hatched region represents the peak in the dynamic correlation length.

reproduction of Holyst and Schick's phase diagram in Fig. 11(b). Although they studied the specific case with  $N_{AB} = N$ , we anticipate that the relative positions of the disorder and Lifshitz lines will be similar in our system ( $N_{AB} \approx 5N$ ). In Fig. 11(b), the total monomer Lifshitz line is completely vertical, whereas the h/h Lifshitz line is closer to horizontal. In addition, all Lifshitz and disorder lines meet at the tricritical Lifshitz point. In our system, the disordered phase region around this putative Lifshitz point appears to be expanded due to the fluctuations. We note that the three experimentally measured lines follow the mean-field theory very well qualitatively for the higher temperature regions, even appearing to converge to a single point. In the PO system,<sup>9</sup> the results are similar; in particular the peak in  $\xi_d$  provides a good indication of the transition to BμE behavior. Interestingly, in this system the BμE channel is not vertical on this plot [Fig. 11(c)], indicating an asymmetry in the temperature dependence of the interactions among the components, whereas in the EED case the channel is, as far as has been discerned so far, vertical. On the basis of these results, then, we propose that  $\xi_d$  peak position follows the h/h Lifshitz line, and clearly delineates between a good microemulsion and an unstructured fluid.

### E. Interfacial structure

The Teubner–Strey model for microemulsions is a Ginzburg–Landau expansion with two gradient terms. Hence one might not expect a good fit to the data at large  $q$  values, where local structural details become important. In fact, various o/w/s systems are well described by the Teubner–Strey form even for reasonably large values of  $q$ . This is a consequence of the  $q^{-4}$  decay characterizing systems with a large amount of interface. The model-independent relation by Porod gives the expected large  $q$  behavior:<sup>29</sup>

$$\lim_{q \rightarrow \infty} I(q)q^4 = 2\pi(\Delta\rho)^2 S, \quad (8)$$

where  $\Delta\rho$  is the difference in scattering length densities and  $S$  is the microemulsion interfacial area per unit volume. At large  $q$  the  $q^{-4}$  term is dominant in the Teubner–Strey model, which is consistent with Porod-type behavior.

To examine the large  $q$  scattering behavior, we took measurements using a sample-to-detector distance of 7 m. Figure 12(a) shows a measurement of the 9.2% sample taken at 85 °C, and Fig. 12(b) the 10% sample at 25 °C. The dashed curves are fits to the Teubner–Strey form; the fits are excellent at low  $q$ , but underestimate the data at high  $q$ . This behavior was noted in other ternary polymeric systems<sup>8</sup> as well as in some o/w/s systems.<sup>30</sup> The high  $q$  behavior could be attributed to Gaussian coil scattering,<sup>8,31</sup> but this explanation is specific to the polymer systems only and is not applicable for the o/w/s case.

The diffuseness of the interface may also affect the large  $q$  scattering behavior. The  $q^{-4}$  dependence assumes sharp interfaces, whereas the experimental scattering density profile may vary more smoothly. Strey *et al.*<sup>32</sup> used a Gaussian term to model this behavior; effectively Eq. (8) is modified by multiplying the right-hand side with  $\exp(-q^2 t^2)$ , where  $t$  is a Gaussian width. This modification agrees well with some

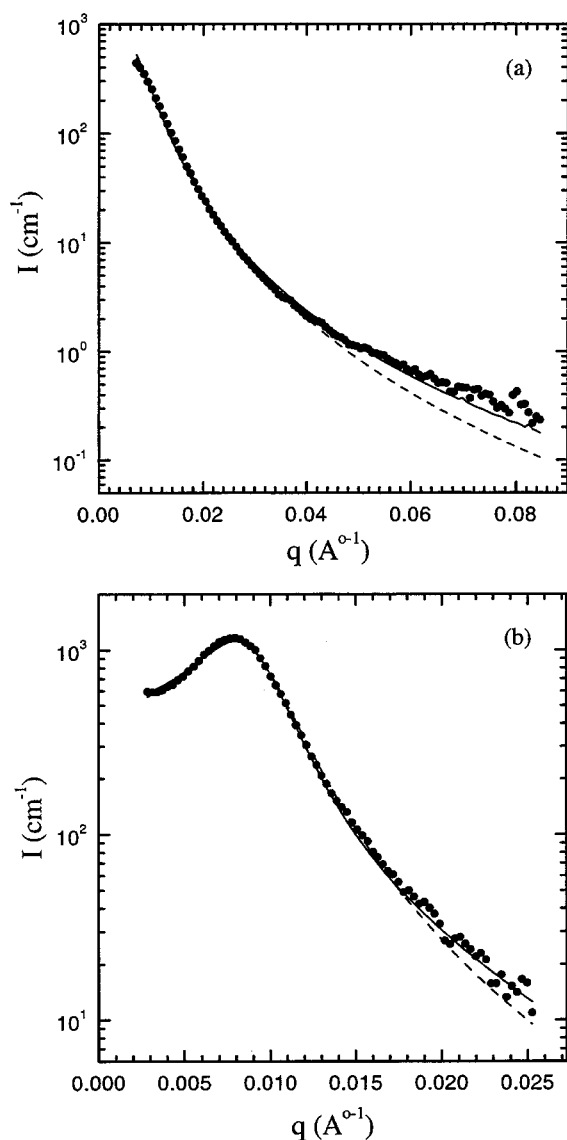


FIG. 12. Comparison of three-parameter fit (solid line) and Teubner–Strey fit (dashed line) for (a) 9.2% EED sample at 85 °C, (b) 10% EED sample at 25 °C.

o/w/s B $\mu$ E and w/s sponge phases.<sup>32</sup> However the diffuse interface model does not explain the observations in the current system, as the Gaussian convolution correction would lead to a steeper decay than that predicted by Teubner–Strey model.

There are other models available for describing the structure factor of the microemulsions. Chen and co-workers<sup>30,33,34</sup> have applied a random wave model, which incorporates the random wave description of Cahn<sup>35</sup> and Berk.<sup>36</sup> Three fitting parameters,  $a$ ,  $b$ , and  $c$  are involved. The first two parameters are directly related to  $d$  and  $\xi$  of the Teubner–Strey fit, as  $a \approx 2\pi/d$  and  $b \approx 1/\xi$ . The third parameter gives a measure of the “persistence length” of the interface, i.e., as  $1/c$ . The mathematics of the model are omitted here as they are complicated; they are available in the original references.<sup>33,34</sup> We applied this three-parameter model to fit our data on the EED samples. Figures 12(a) and 12(b) show the fits using this model as compared to the

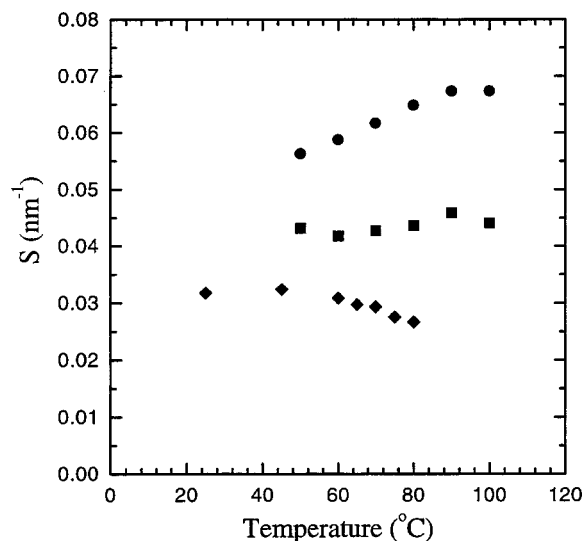


FIG. 13. Surface area per unit volume as a function of temperature for EED samples with 10% (●), 12% (■), and 15% (◆) block copolymer.

Teubner–Strey fits. The random wave model gives an improved fit at large  $q$ . The comparison is clearer in the case of the 9.2% sample, where more data were collected at large  $q$ . The aforementioned correspondence of the fitting parameters  $a$  and  $b$  to the Teubner–Strey parameters was found to be valid for our system.

The models discussed above can be used to obtain structural details such as surface area per unit volume ( $S$ ) and interfacial curvature. Equation (8) indicates that  $S$  can be calculated from the scattered intensity in the large  $q$  limit. Although we observe deviations from  $q^{-4}$  decay at large  $q$ , there is an intermediate region where Porod-type behavior is observed. Hence a rough estimate of  $S$  can be obtained using Eq. (8). Figure 13 shows the results for the EED system. The surface area per unit volume is a weak function of temperature, but strongly increases with copolymer volume fraction. This is consistent with the behavior of the domain spacing  $d/2$  shown in Fig. 6(b); the increase in  $S$  is coincident with the decrease in  $d$ .

Theoretical models for bicontinuous microemulsions relate  $\xi$  to the total interfacial area per unit volume as

$$\xi = \frac{\alpha \phi_1 \phi_2}{S}, \quad (9)$$

where  $\phi_i$  is the volume fraction of component  $i$ , and  $\alpha$  is a topological parameter calculated to be between 4 and 6. The Teubner–Strey model, for example, gives  $\alpha=4$ . Sottmann *et al.*<sup>37</sup> have found  $\xi_{TS} \approx d_{TS}/2$  for a wide range of o/w/s mixtures, and thus identify  $\xi$  in Eq. (9) with either  $\xi_{TS}$  or  $d_{TS}/2$ . They have also measured the value  $\alpha=7.16$  for these mixtures at the “fish tail” point (i.e., the boundary between microemulsion and multiphase equilibria on the temperature/amphiphile concentration plot<sup>38</sup>).

In our polymeric system, in general,  $\xi_{TS}$  is not equal to  $d_{TS}/2$ , but the values are closest deep in the microemulsion channel. Chen *et al.*<sup>39</sup> have reported that  $\xi_{TS}/d_{TS}$  is a measure of the domain size polydispersity: the smaller the ratio, the larger the polydispersity. Hence the difference between

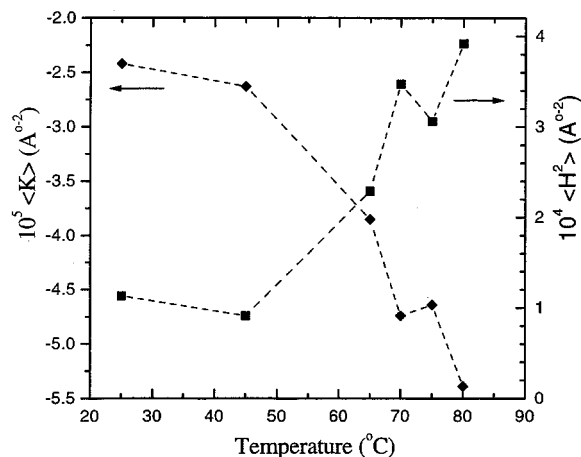


FIG. 14. Gaussian curvature  $\langle K \rangle$  (●) and mean square curvature  $\langle H^2 \rangle$  (■) calculated from the three-parameter model for the EED sample, as a function of temperature.

$\xi_{TS}$  and  $d_{TS}/2$  can probably be attributed to a much larger domain size polydispersity in the polymer B $\mu$ E than in the typical o/w/s systems. We use Eq. (8) to calculate  $S = 0.032 \text{ nm}^{-1}$  for the 10% mixture at room temperature. From Eq. (9), we then calculate a value of  $\alpha$  of either 4.9 or 5.8 from  $\xi$  equal to  $\xi_{TS}$  or  $d_{TS}/2$ , respectively. These values are closer to that expected by theory. The smaller value for  $\alpha$  than in the o/w/s system shows a more efficient use of interfacial area to form domains in the polymer system. The area of the internal interface is itself related to the area per block copolymer molecule,  $a_{bc}$ , by  $S = \phi_{bc} a_{bc} / v_{bc}$ , where  $v_{bc}$  is the volume of a block copolymer molecule, estimated to be  $19 \text{ nm}^3$ . This gives an area per block copolymer molecule at the interface of about  $6.5 \text{ nm}^2$ . This is much larger than the typical value of  $0.5 \text{ nm}^2$  for a nonionic surfactant, but is reasonable for this polymer system.

The random wave model of Chen *et al.* can also be used to calculate the mean square and Gaussian curvatures of the bicontinuous microemulsion.<sup>33,34,39</sup> The mean curvature of a bicontinuous microemulsion is zero. Hence the mean square curvature is the variance of the fluctuations of the mean curvature. The Gaussian curvature is the product of the two principal curvatures at any point on the surface. Since the interface is saddlelike at most places, we may expect the Gaussian curvature to be negative. Choi and Chen have derived algebraic expressions for the Gaussian curvature  $\langle K \rangle$  and the mean square curvature  $\langle H^2 \rangle$  of the microemulsion as functions of the three fitting parameters.<sup>34</sup> We calculated these curvatures using their model; the results for the 10% sample are presented in Fig. 14. It is observed that the absolute value of the curvature increases with temperature. This is because the interfaces of the microemulsion tend to become flatter with decreasing temperature, as the system approaches the lamellar phase. As noted previously a measure of the persistence length of the interface can be obtained from the reciprocal of the third fitting parameter  $c$ . The persistence length is found to increase with decreasing temperature consistent with the curvature.

## V. SUMMARY

We have investigated the static and dynamic behavior of the disordered phase in two ternary polymer blend systems. A low temperature channel of polymeric bicontinuous microemulsion (B $\mu$ E) is found in each case. The SANS measurements are interpreted via the Teubner–Strey structure factor, and it describes the disordered phase structures well, with some systematic deviations at high  $q$ . SANS measurements indicate that the disorder line and the total monomer Lifshitz line are vertical except over a small temperature interval near the opening of the B $\mu$ E channel. DLS results show that the dynamic correlation length increases in size in the disordered phase with decreasing temperature, peaks at the onset of the B $\mu$ E phase, and decreases with further increasing temperature. This dynamic signature of the poorly structured to good microemulsion transition appears to be the clearest demarcation of the onset of B $\mu$ E behavior. Furthermore, the transition is apparently most strongly correlated with the homopolymer/homopolymer Lifshitz line, but this inference could be tested with different deuterium-labeling schemes. In contrast to oil/water/surfactant systems, the disorder line and total monomer Lifshitz line do not signify different microemulsion structures, but instead simply signify regions of varying amphiphilicity.

## ACKNOWLEDGMENTS

This work was supported in part by the MRSEC program of the National Science Foundation under Award No. DMR-9809364, by the Center for Interfacial Engineering, a NSF-sponsored Engineering Research Center at the University of Minnesota, and by the Grant Agency of the Academy of Sciences of the Czech Republic (Award No. A1050902 to P.S.). The support and assistance of the staff of the NIST SANS facility is particularly appreciated. We thank Kristoffer Almdal, Ken Hanley, and Newell Washburn for assistance with the SANS measurements and David Morse for helpful discussions.

- <sup>1</sup>G. Gompper and M. Schick, *Self-Assembling Amphiphilic Systems* (Academic, New York 1994).
- <sup>2</sup>*Micelles, Membranes, Microemulsions, and Monolayers*, edited by W. M. Gelbart, A. Ben-Shaul, and D. Roux (Springer, New York, 1994).
- <sup>3</sup>F. S. Bates, *Science* **251**, 898 (1991).
- <sup>4</sup>L. E. Scriven, *Nature (London)* **63**, 123 (1976).
- <sup>5</sup>M. Teubner and R. Strey, *J. Chem. Phys.* **87**, 3195 (1987).
- <sup>6</sup>M. Kahlweit *et al.*, *J. Colloid Interface Sci.* **118**, 436 (1987).
- <sup>7</sup>F. S. Bates, W. W. Maurer, P. M. Lipic, M. A. Hillmyer, K. Almdal, K. Mortensen, G. H. Fredrickson, and T. P. Lodge, *Phys. Rev. Lett.* **79**, 849 (1997).
- <sup>8</sup>M. A. Hillmyer, W. W. Maurer, T. P. Lodge, F. S. Bates, and K. Almdal, *J. Phys. Chem. B* **103**, 4814 (1999).
- <sup>9</sup>N. R. Washburn, T. P. Lodge, and F. S. Bates, *J. Phys. Chem. B* **104**, 6987 (2000).
- <sup>10</sup>T. L. Morkved, B. R. Chapman, F. S. Bates, T. P. Lodge, P. Stepanek, and K. Almdal, *Faraday Discuss.* **112**, 335 (1999).
- <sup>11</sup>D. Broseta and G. H. Fredrickson, *J. Chem. Phys.* **93**, 2927 (1990).
- <sup>12</sup>R. Holyst and M. Schick, *J. Chem. Phys.* **96**, 7728 (1992).
- <sup>13</sup>P. K. Janert and M. Schick, *Macromolecules* **30**, 3916 (1997).
- <sup>14</sup>L. Kielhorn and M. Muthukumar, *J. Chem. Phys.* **107**, 5588 (1997).
- <sup>15</sup>M. W. Matsen, *J. Chem. Phys.* **110**, 4658 (1999).
- <sup>16</sup>D. Schwahn, K. Mortensen, H. Frielinghaus, and K. Almdal, *Phys. Rev. Lett.* **82**, 5056 (1999).



- <sup>17</sup>D. Schwahn, K. Mortensen, H. Frielinghaus, K. Almdal, and L. Kielhorn, J. Chem. Phys. **112**, 5454 (2000).
- <sup>18</sup>K.-V. Schubert and R. Strey, J. Chem. Phys. **95**, 8532 (1991).
- <sup>19</sup>K.-V. Schubert, R. Strey, S. R. Kline, and E. W. Kaler, J. Chem. Phys. **101**, 5343 (1994).
- <sup>20</sup>R. D. Koehler, K.-V. Schubert, R. Strey, S. R. Kline, and E. W. Kaler, J. Chem. Phys. **101**, 10843 (1994).
- <sup>21</sup>G. Gompper and M. Schick, Phys. Rev. Lett. **65**, 1116 (1990).
- <sup>22</sup>M. A. Hillmyer and F. S. Bates, Macromolecules **29**, 6994 (1996).
- <sup>23</sup>J. D. Ferry, *Viscoelastic Properties of Polymers*, 3rd ed. (Wiley, New York, 1980).
- <sup>24</sup>J. Jakes, Collect. Czech. Chem. Commun. **60**, 1781 (1995).
- <sup>25</sup>F. S. Bates, J. H. Rosedale, P. Stepanek, T. P. Lodge, P. Wiltzius, G. H. Fredrickson, and R. P. Hjelm, Phys. Rev. Lett. **65**, 1893 (1990).
- <sup>26</sup>P. Stepanek, T. P. Lodge, C. Kedrowski, and F. S. Bates, J. Chem. Phys. **94**, 8289 (1991).
- <sup>27</sup>G. Meier, B. Momper, and E. W. Fischer, J. Chem. Phys. **97**, 5884 (1992).
- <sup>28</sup>D. Schwahn, G. Meier, K. Mortensen, and S. Janssen, J. Phys. II **4**, 837 (1994).
- <sup>29</sup>G. Porod, in *Small Angle X-ray Scattering*, edited by O. Glatter and O. Kratky (Academic, New York, 1982).
- <sup>30</sup>H. Jinnai, T. Hashimoto, D. Lee, and S.-H. Chen, Macromolecules **30**, 130 (1997).
- <sup>31</sup>J. S. Higgins and H. C. Benoit, *Polymers and Neutron Scattering* (Clarendon, Oxford, 1994).
- <sup>32</sup>R. Strey, J. Winkler, and L. Magid, J. Phys. Chem. **95**, 7502 (1991).
- <sup>33</sup>S.-H. Chen, D. Lee, and S.-L. Chang, J. Mol. Struct. **296**, 259 (1993).
- <sup>34</sup>S.-M. Choi and S.-H. Chen, Prog. Colloid. Polym. Sci. **106**, 14 (1997).
- <sup>35</sup>J. W. Cahn, J. Chem. Phys. **42**, 93 (1965).
- <sup>36</sup>N. F. Berk, Phys. Rev. Lett. **58**, 2718 (1987).
- <sup>37</sup>T. Sottmann, R. Strey, and S.-H. Chen, J. Chem. Phys. **106**, 6483 (1997).
- <sup>38</sup>M. Kahlweit, R. Strey, D. Hasse, and P. Firman, Langmuir **4**, 785 (1988).
- <sup>39</sup>S.-H. Chen, S. L. Chang, and R. Strey, Prog. Colloid Polym. Sci. **81**, 30 (1990).